Ammonia IRMS-TPD for Measurements of Number and Strength of Brønsted and Lewis Acid Sites

Naonobu Katada, Yuya Kawatani, Kana Yamamoto, Satoshi Suganuma and Etsushi Tsuji
Center for Research on Green Sustainable Chemistry, Tottori University, 4-101 Koyama-cho Minami, Tottori 680-8552, Japan
katada@tottori-u.ac.jp

Introduction

Here the ammonia IRMS (infrared-mass spectroscopy)-TPD (temperature-programmed desorption)[1] was applied to the samples. The method was developed by combining the conventional ammonia TPD and IR techniques to measure the number and strength of Brønsted and Lewis acid sites on a solid, and recently the accuracy has been improved by developing an automatic analyzer[2].

Experimental

As shown in our previous paper[3], ca. 6 mg of the powder sample was compressed into a self-supporting thin wafer with 1 cm of the diameter. In an operando analyzer (MicrotracBEL, IRMS-TPD), it was pre-treated in flowing oxygen (102 kPa, 33 μmol s^{-1}) at 823 K for 90 min. The IR spectra of thus pre-treated zeolite were measured with 1 K of the interval in flowing inert gas (helium or argon, 5.5 kPa, 81 μmol s^{-1}) with elevating the temperature from 313 to 813 K at 0.033 K s^{-1}. Then, ammonia (13 kPa) was admitted contacting to the sample at 313 K for 30 min. After stabilization in the inert gas flow (5.5 kPa, 81 μmol s^{-1}), the sample was again heated from 313 to 813 K at 0.033 K s^{-1} with recording the IR spectra at 1 K interval and MS ion currents. After the measurements, the intensity of MS was calibrated with ammonia / helium (or argon) mixture with known concentration.

Thus, MS-TPD profile, i.e., plots of concentration of ammonia in gas phase (C_g) against the temperature (T) was obtained, as well as the difference IR spectra of adsorbed ammonia (spectrum after the adsorption of ammonia − that before the adsorption of ammonia measured at the same temperature) at elevated temperatures. Differentiation of the peak intensities (peak areas) of symmetric deformation of NH_4 held by Brønsted acid site (1450 cm^{-1}) and NH_3→Al on Lewis acid site (1300 cm^{-1}) gave the IR-TPD, namely, the plots of $-dA_i/dT$ against T, where A_i shows the absorbance of species i (i = NH_4 or NH_3→Al) in the difference IR spectrum. It is here assumed that the sum of desorption rates of ammonia from Brønsted and Lewis acid sites equals to the total desorption rate reflected by C_g. Based on this assumption, the curve fitting between $k_{NH4}(-dA_{NH4}/dT)+k_{NH3\rightarrow Al}(-dA_{NH3\rightarrow Al}/dT)$ and C_g to find the pair of k_{NH4} and $k_{NH3\rightarrow Al}$ giving the best fitting over the experimental temperature range was carried out. The thus calculated k_i of the species i shows $\pi d^2\beta/4\varepsilon_i F$, where π, d, β and F show the circle ratio (3.14), diameter of the wafer (10 mm), ramp rate (0.033 K s^{-1}) and apparent flow rate of carrier gas (1.50×10^{-5} m^3 s^{-1}). The parameter ε_i is the molar extinction coefficient of the discussed species i, which has been unknown before the measurement, but here thus estimated. Simultaneously, the plots of $k_{NH4}(-dA_{NH4}/dT)$ and $k_{NH3\rightarrow Al}(-dA_{NH3\rightarrow Al}/dT)$ against T are obtained. These should be the plots of C_g desorbed from each of Brønsted and Lewis acid sites as functions of T, i.e., the ammonia IRMS-TPD profiles from each of Brønsted and Lewis acid sites[3].

The acid amount (A_0) is calculated by $\int FC_g dt/W$ [$=\int FC_g dT/(\beta W)$], where t and W are the time and amount the zeolite wafer, measured after the experiment. As an index of acid strength, the molar standard enthalpy of ammonia desorption (ΔH^o) and its distribution was calculated by a curve fitting method[4,5] according to the theoretical equation[6] $C_g = -A_0 W/F(d\theta/dt) = \theta P^o e^{-\Delta H^o/(RT)} e^{\Delta S^o/R}/\{(1-\theta)RT\}$, where e, θ, P^o, R and ΔS^o are the Napier's constant (2.72), coverage of acid site by ammonia, pressure in the standard conditions (10^5 Pa), gas constant (8.314 J K^{-1} mol^{-1}) and molar standard entropy of ammonia desorption (assumed to be 155 J K^{-1} mol^{-1} based on the experiments[6–8]).

Results

As shown in Figure 1, IRZ-FAU001, IRZ-MFI001 and IRZ-MFI002 revealed IR spectra of typical zeolites which consisted of bands at 3745 cm^{-1} due to isolated SiOH on the external surface and those at 2000, 1860, 1765, 1540 and ca. 1100 cm^{-1} (very strong) ascribable to SiO framework, as well as some noises due to H_2O and CO_2. In addition, IRZ-MFI001 and IRZ-MFI002, the MFI samples with high Al concentration showed 3610 cm^{-1}-band due to the Brønsted acidic AlOHSi, whereas IRZ-FAU001, the FAU sample showed those at 3625 and 3580 cm^{-1}, attributed to the AlOHSi in supercage and sodalite cage[9], respectively. IRZ-MFI003, the MFI sample with low Al concentration showed a broad absorption due to OH stretching in 2500−3800 cm^{-1} region, but no clear band ascribable to the Brønsted acidic AlOHSi was observed.

As shown in Figure 2, the IR spectra of adsorbed ammonia revealed the symmetric deformation of NH_4 bonded to Brønsted acid site (1450 cm^{-1}) on all samples, while the symmetric deformation of $NH_3 \rightarrow Al$ as a Lewis acid site (1300 cm^{-1}) was small, especially on MFI (IRZ-MFI001, IRZ-MFI002 and IRZ-MFI003). These bands were deconvoluted as Figure 3, and the temperature dependences of band intensities were analyzed. On the other hand, the mass spectrometer gave the change in NH_3 concentration in the gas phase. They were totally analyzed to provide the TPD profiles of Brønsted and Lewis acid sites as shown in Figure 4. The amounts of Brønsted and Lewis acid sites were estimated from the peak intensities of these profiles as shown in Table 1. Distribution of ammonia desorption enthalpy (close to energy), an index of acid strength, was analyzed by means of an analytical method[5] based on the curve-fittings in Figure 5 and Figure 6 to give the distribution curves shown in Figure 7.

Figure 7 shows that the enthalpy of ammonia desorption of most Brønsted acid sites on MFI (IRZ-MFI001, IRZ-MFI002 and IRZ-MFI003) was 130−150 kJ mol^{-1}, as typically observed on MFI type aluminosilicates without extra-framework cations[2,4]. On the other hand, the FAU sample (IRZ-FAU001) had weak (enthalpy = 110−115 kJ mol^{-1}) and strong (120−145 kJ mol^{-1}) fractions of Brønsted acid strength. The former is attributed to the Brønsted acid sites generated by isomorphous substitution of Si with Al in the FAU framework[9], while the latter is speculated to be the Brønsted acid site enhanced by extra-framework $AlOH^{2+}$ cation located near to the site[10–14]. Figure 7 also shows the enthalpy of ammonia desorption of Lewis acid sites. Again the relatively large amount of Lewis acid sites on the FAU sample (IRZ-FAU001) is found.

The amounts of Brønsted acid sites are summarized in Table 2 as well as the chemical compositions. The NH_4-MFI sample with high Al concentration (IRZ-MFI002) had a large amount of Brønsted acid sites, corresponding to 0.982, close to 1, of [Al] - [Na] contents, indicating generation of Brønsted acid site by the isomorphous substitution of Si with Al. On the other hand, the ratio [Brønsted acid] / ([Al] − [Na]) was lower, 0.799, on the H-MFI (IRZ-MFI001) with Al content similar to that of IRZ-MFI002. IRZ-MFI001 was prepared by calcination to remove NH_3 from an NH_4-MFI equivalent to IRZ-MFI002. Calcination and storage in atmosphere of H-MFI with high Al concentration was thus found to decrease the ion exchange capacity, presumably due to dealumination from Al-rich proton-form zeolite in humid atmosphere even at room temperature, while NH_4-form was stable as reported[15–17]. On the other hand, the H-MFI sample with low Al concentration showed only 0.2, far smaller than 1, of the [Brønsted acid] / ([Al] − [Na]) ratio, indicating the presence of considerable amount of extra-framework Al. In this case, the calcination and exposure of H-form to the atmosphere was not the cause of dealumination, because the Al concentration was low. The FAU sample (IRZ-FAU001) also showed low the [Brønsted acid] / ([Al] − [Na]) ratio, 0.30. In addition to the detection of Brønsted acid site enhanced by the extra-framework Al species as above, this points out the presence of considerable amount of extra-framework Al on IRZ-FAU001.

Figure 8 compares the ammonia desorption enthalpy distributions of Brønsted acid sites on the present samples and *BEA, MWW, YFI and MOR zeolites. This tells us that the Brønsted acid strength was different among zeolites with different framework topologies. The reason has been discussed[18].

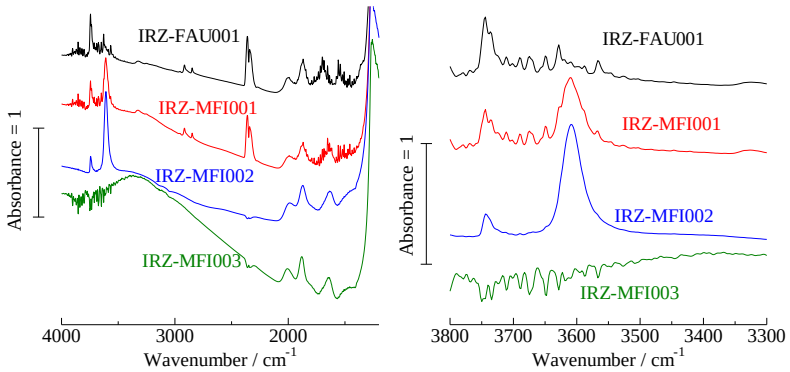

Data table: (0.1MB)

Figure 1: Infrared spectra of pre-treated zeolites at 373 K. The right-hand side shows the enlarged portion.

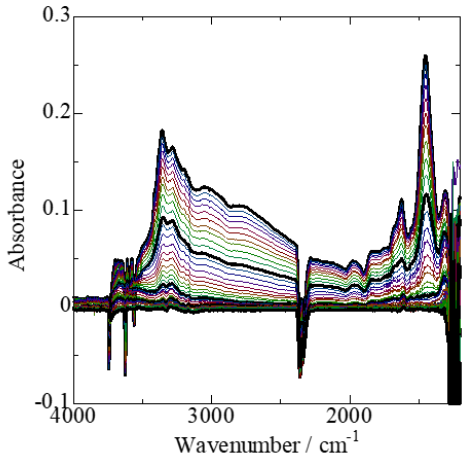

IRZ-FAU001

Data table at 10 K interval: (2.5MB)

Data table all: (10.9MB)

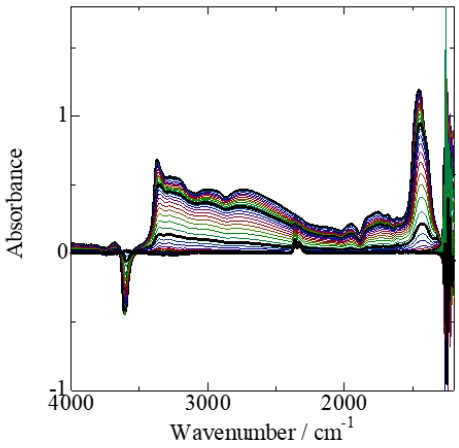

IRZ-MFI001

Data table at 10 K interval: (2.4MB)

Data table all: (10.6MB)

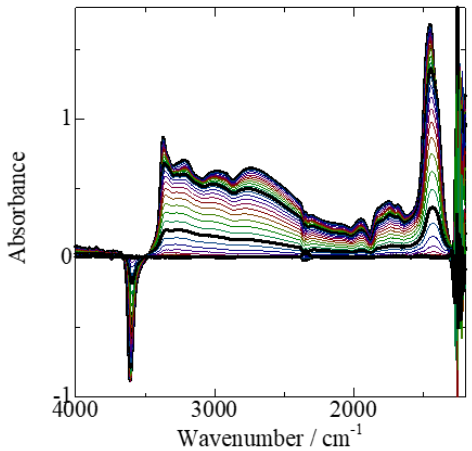

IRZ-MFI002

Data table at 10 K interval: (3.9MB)

Data table all: (10.6MB)

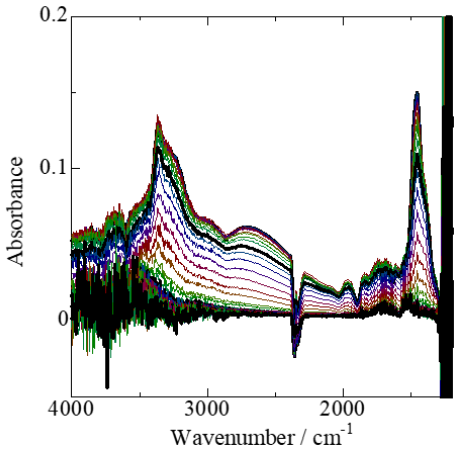

IRZ-MFI003

Data table at 10 K interval: (2.4MB)

Data table all: (10.6MB)

Figure 2: [Absorbance after ammonia adsorption] – [Absorbance before ammonia adsorption] at elevated temperatures. Thick black lines show the spectra at 373, 473, 573, 673 and 773 K, and the thin lines show the spectra at 10 K of the interval. The thick black line at the most upper position in 2500−3300 cm^{-1} region is the spectra at 373 K.

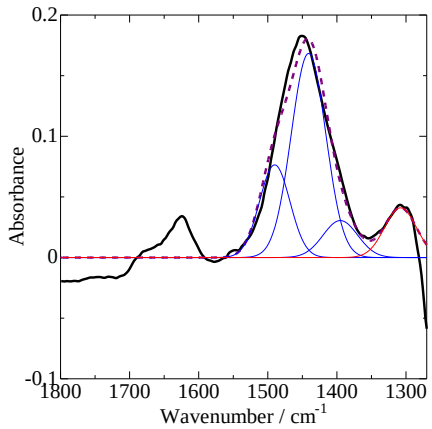

IRZ-FAU001 Data table: (0.07MB)

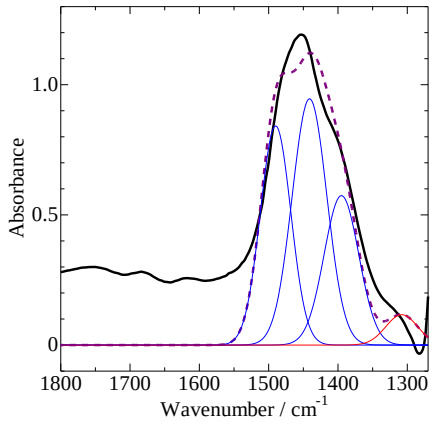

IRZ-MFI001 Data table: (0.07MB)

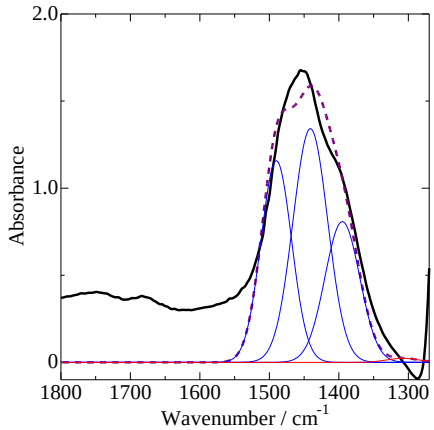

IRZ-MFI002 Data table: (0.07MB)

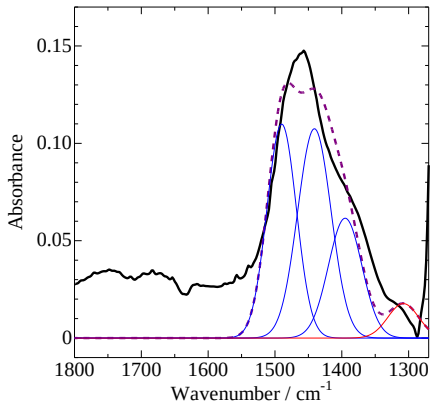

IRZ-MFI003 Data table: (0.07MB)

Figure 3: Deconvolution of symmetric deformation band of adsorbed species at 373 K. The thick black line shows the observed spectrum. The blue lines show the simulated band due ascribed to ν_4 vibration of NH_4 formed by the reaction between Brønsted acid site and ammonia. The red line shows the simulated band ascribed to δ_s vibration of NH_3-Al species formed by the reaction between Lewis acid site and ammonia[19]. The dotted purple line showed the sum of simulated bands.

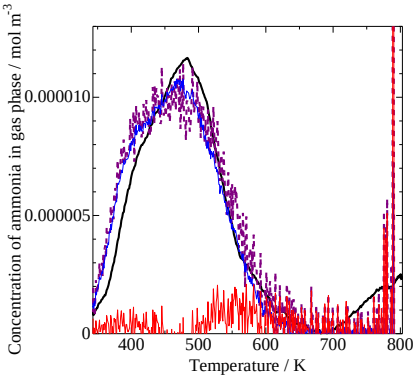

IRZ-FAU001 Data table: (0.05MB)

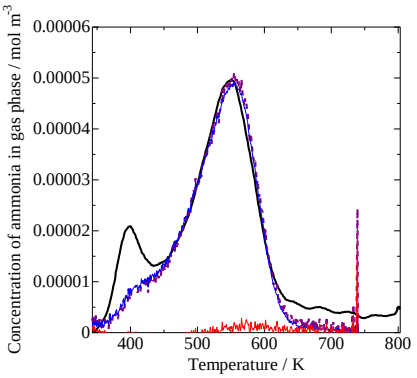

IRZ-MFI001 Data table: (0.05MB)

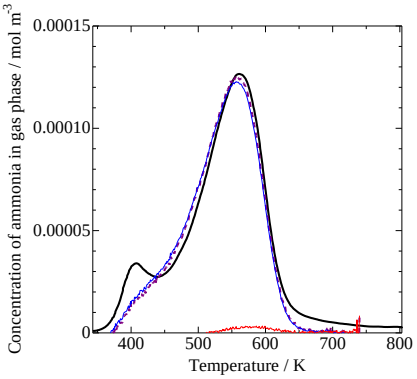

IRZ-MFI002 Data table: (0.05MB)

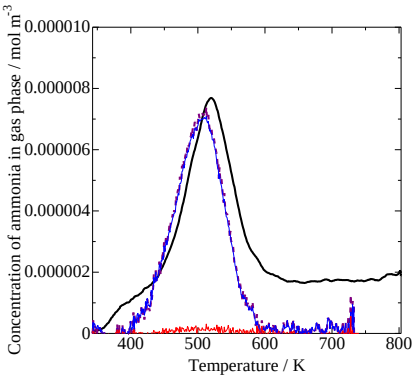

IRZ-MFI003 Data table: (0.05MB)

Figure 4: Ammonia TPD profiles of total (black), Brønsted (blue) and Lewis (red) acid sites.

Table 1: Brønsted and Lewis acid amounts calculated from areas of TPD peaks. Significant digits are up to two decimal places, but for convenience, all digits are written.

Sample	Acid amount / mol kg^{-1}	
	Brønsted	Lewis
IRZ-FAU001	0.303354388	0.031764668
IRZ-MFI001	1.042975611	0.018365303
IRZ-MFI002	1.317670894	0.001929321
IRZ-MFI003	0.074501068	0.001304755

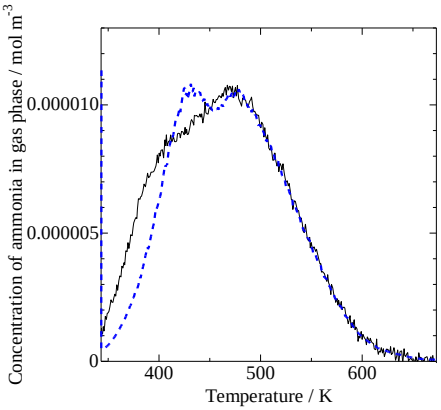

IRZ-FAU001 Data table: (0.04MB)

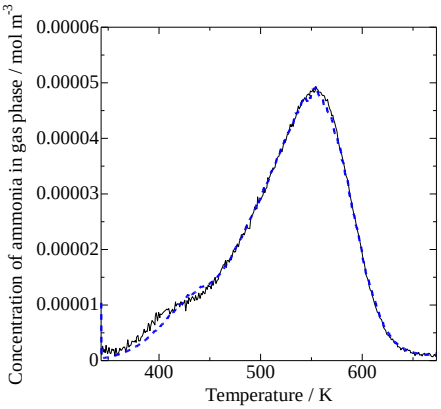

IRZ-MFI001 Data table: (0.04MB)

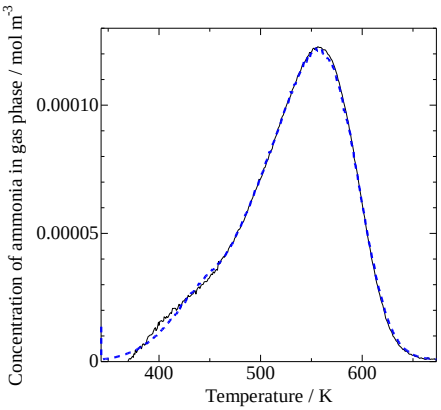

IRZ-MFI002 Data table: (0.04MB)

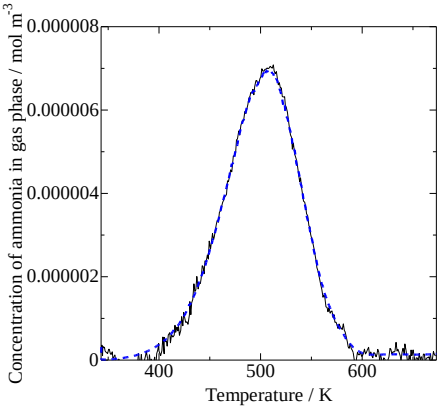

IRZ-MFI003 Data table: (0.04MB)

Figure 5: Ammonia TPD profiles of Brønsted acid site observed (solid line) and simulated (dotted line) based on assumed distribution of desorption enthalpy.

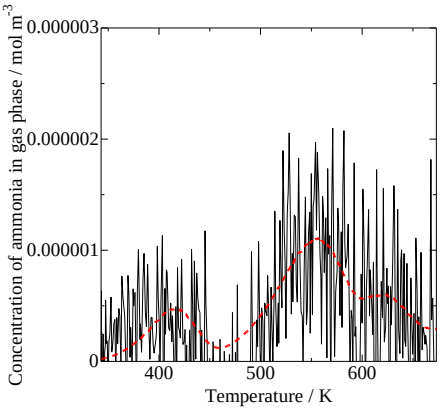

IRZ-FAU001 Data table: (0.04MB)

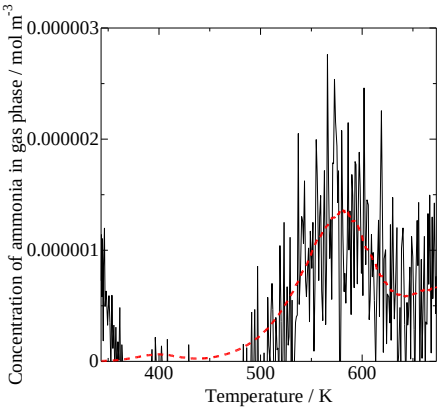

IRZ-MFI001 Data table: (0.04MB)

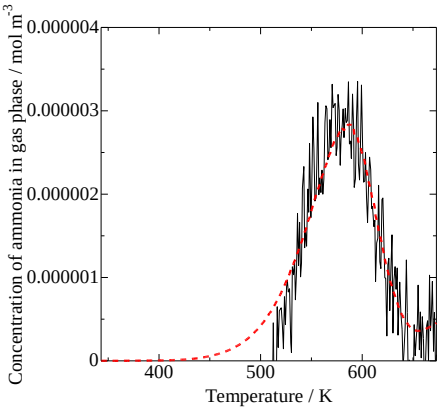

IRZ-MFI002 Data table: (0.04MB)

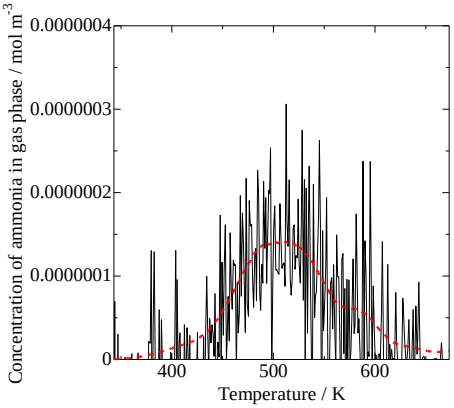

IRZ-MFI001 Data table: (0.04MB)

Figure 6: Ammonia TPD profiles of Lewis acid site observed (solid line) and simulated (dotted line) based on assumed distribution of desorption enthalpy.

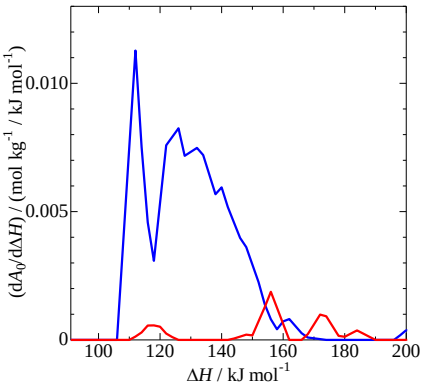

IRZ-FAU001 Data table: (0.01MB)

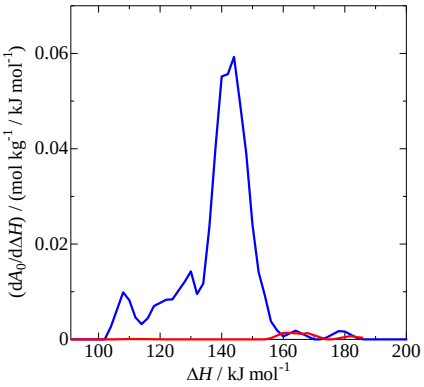

IRZ-MFI001 Data table: (0.01MB)

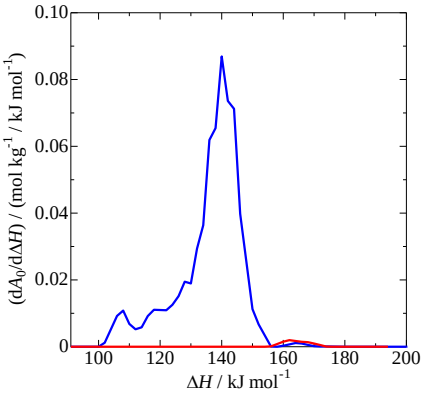

IRZ-MFI002 Data table: (0.01MB)

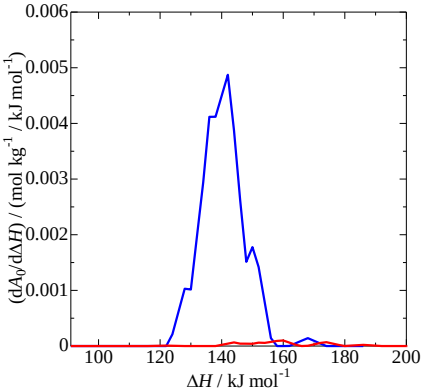

IRZ-MFI003 Data table: (0.01MB)

Figure 7: Distribution of enthalpy of ammonia desorption from Brønsted (blue) and Lewis (red) acid sites. The plots was modified with smoothing.

Table 2: Chemical composition and parameters of acidic property

Sample	[Si] / [Al]	[Al] / mol kg^{-1}	[Na] / mol kg^{-1}	([Al] − [Na]) / mol kg^{-1}	[B acid] / mol kg^{-1}	[L acid] / mol kg^{-1}	[B acid] / ([Al] − [Na])
IRZ-FAU001	30	1.05	0.032	1.02	0.30	0.03	0.30
IRZ-MFI001	23.8	1.31	<0.004	1.31	1.04	0.02	0.799
IRZ-MFI002	23.1	1.34	<0.003	1.34	1.32	0.00	0.982
IRZ-MFI003	100	0.33	unreported	0.33*	0.07	0.00	0.2

*: [Na] is assumed to be zero.

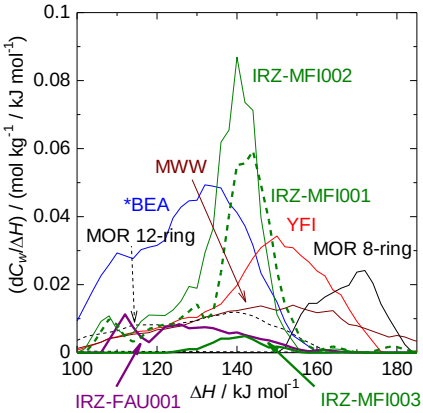

Data table: (0.01MB)

Figure 8: Distributions of ammonia desorption enthalpy of Brønsted acid sites on various zeolites. The data on *BEA, MOR, YFI and MWW are taken from a recent paper[20]. On MOR, the ammonia desorption enthalpies of Brønsted sites in 8- and 12-ring are separately analyzed, because the OH stretching bands are identified in IR spectrum. The plots was modified with smoothing.

[1] M. Niwa and N. Katada, *Chem. Rec.*, **13**, 432 (2013). https://doi.org/10.1002/tcr.201300009
[2] N. Katada, *Mol. Catal.*, **458**, 116 (2018). https://doi.org/10.1016/j.mcat.2017.12.024
[3] M. Niwa, K. Suzuki, N. Katada, T. Kanougi and T. Atoguchi, *J. Phys. Chem., B*, **109**, 18749 (2005). https://doi.org/10.1021/jp051304g
[4] N. Katada, H. Igi, J.-H. Kim and M. Niwa, *J. Phys. Chem., B*, **101**, 5969 (1997). https://doi.org/10.1021/jp9639152
[5] N. Katada, T. Tsubaki and M. Niwa, *Appl. Catal., A: Gen.*, **340**, 76 (2008). https://doi.org/10.1016/j.apcata.2008.01.033
[6] M. Niwa, N. Katada, M. Sawa and Y. Murakami, *J. Phys. Chem.*, **99**, 8812 (1995). https://doi.org/10.1021/j100021a056
[7] N. Naito, N. Katada and M. Niwa, *J. Phys. Chem., B*, **103**, 7206 (1999). https://doi.org/10.1021/jp9906381
[8] N. Katada, J. Endo, K. Notsu, N. Yasunobu, N. Naito and M. Niwa, *J. Phys. Chem., B*, **104**, 10321 (2000). https://www.doi.org/10.1021/jp002212o
[9] K. Suzuki, N. Katada and M. Niwa, *J. Phys. Chem., C*, **111**, 894 (2007). https://doi.org/10.1021/jp065054v
[10] N. Katada, Y. Kageyama, K. Takahara, T. Kanai, H. A. Begum and M. Niwa, *J. Mol. Catal., A: Chem.*, **211**, 119 (2004). https://doi.org/10.1016/j.molcata.2003.10.001
[11] N. Katada, S. Nakata, S. Kato, K. Kanehashi, K. Saito and M. Niwa, *J. Mol. Catal., A: Chem.*, **236**, 239 (2005). https://doi.org/10.1016/j.molcata.2005.04.024
[12] M. Niwa, K. Suzuki, K. Isamoto and N. Katada, *J. Phys. Chem., B*, **110**, 264 (2006). https://doi.org/10.1021/jp054442e
[13] K. Suzuki, T. Noda, G. Sastre, N. Katada and M. Niwa, *J. Phys. Chem., C*, **113**, 5672 (2009). https://doi.org/10.1021/jp8104562
[14] K. Okumura, T. Tomiyama, N. Morishita, T. Sanada, K. Kamiguchi, N. Katada and M. Niwa, *Appl. Catal., A: Gen.*, **405**, 8 (2011). https://doi.org/10.1016/j.apcata.2011.07.007
[15] N. Katada, Y. Kageyama and M. Niwa, *J. Phys. Chem., B*, **104**, 7561 (2000). https://doi.org/10.1021/jp000906r
[16] N. Katada, T. Kanai and Miki Niwa, *Micropor. Mesopor. Mater.*, **75**, 61 (2004). https://doi.org/10.1016/j.micromeso.2004.07.001
[17] N. Katada, T. Takeguchi, T. Suzuki, T. Fukushima, K. Inagaki, S. Tokunaga, H. Shimada, K. Sato, Y. Oumi, T. Sano, K. Segawa, K. Nakai, H. Shoji, P. Wu, T. Tatsumi, T. Komatsu, T. Masuda, K. Domen, E. Yoda, J. N. Kondo, T. Okuhara, Y. Kageyama, M. Niwa, M. Ogura, M. Matsukata, E. Kikuchi, N. Okazaki, M. Takahashi, A. Tada, S. Tawada, Y. Kubota, Y. Sugi, Y. Higashio, M. Kamada, Y. Kioka, K. Yamamoto, T. Shouji, Y. Arima, Y. Okamoto and H. Matsumoto, *Appl. Catal., A: Gen.*, **283**, 63 (2005). https://doi.org/10.1016/j.apcata.2004.12.036
[18] N. Katada, K. Suzuki, T. Noda, G. Sastre and M. Niwa, *J. Phys. Chem., C*, **113**, 19208 (2009). https://doi.org/10.1021/jp903788n
[19] S. Suganuma, Y. Murakami, J. Ohyama, T. Torikai, K. Okumura and N. Katada, *Catal. Lett.*, **145**, 1904 (2015). https://doi.org/10.1007/s10562-015-1592-6
[20] N. Katada, K. Yamamoto, M. Fukui, K. Asanuma, S. Inagaki, K. Nakajima, S. Suganuma, E. Tsuji, A. Palcic, V. Valtchev, P. St. Petkov, K. Simeonova, G. N. Vayssilov and Y. Kubota, *Micropor. Mesopor. Mater.*, **330**, 111592 (2022). https://doi.org/10.1016/j.micromeso.2021.111592